Manuscript submitted to
AIMS' Journals
Volume **X**, Number **0X**, XX **200X**

doi:10.3934/xx.xx.xx.xx

pp. **X–XX**

DIAMOND–CELL FINITE VOLUME SCHEME FOR THE HESTON MODEL

Pavol Kútik

Department of Mathematics
Slovak University of Technology
Radlinského 11, 813 68 Bratislava, Slovakia

Karol Mikula

Department of Mathematics
Slovak University of Technology
Radlinského 11, 813 68 Bratislava, Slovakia

Abstract. The objective of this article is to propose a novel numerical scheme for solving the partial differential equation arising in the Heston stochastic volatility model. We discretize the governing advection-diffusion-reaction equation using the finite volume technique. The diffusion tensor is treated by means of the diamond–cell approximation. A theoretical result concerning the existence and uniqueness of the solution to the corresponding system of linear equations is proved. Numerical experiments regarding accuracy and order of convergence are shown.

1. **Introduction.** The classical Black-Scholes model (cf. [2, 16]) assumes the underlying asset $S > 0$ to follow the geometric Brownian motion $dS = \mu S dt + \sigma S dw$ while the volatility $\sigma > 0$ is constant. However, empirical evidence suggests (cf. [3]) that it is necessary to relax the volatility restriction and allow it to follow a stochastic process as well. One of the stochastic volatility models, introduced by Heston (cf. [12]) uses a mean reverting square root process, originally proposed by Cox, Ingersoll and Ross (cf. [5]), to capture the dynamics of the underlying's variance $v > 0$:

$$dS = \mu S dt + \sqrt{v} S dw, \tag{1}$$

$$dv = \kappa(\theta - v)dt + \sigma\sqrt{v} dz \tag{2}$$

Processes w and z are Wiener stochastic processes mutually correlated by $\mathbb{E}[dwdz] = \rho dt$. The list of other parameters reads as follows: $\rho \in [-1, 1]$ is the correlation parameter, $\kappa > 0$ is the reversion speed, $\sigma > 0$ is the volatility of variance, $\theta > 0$ denotes the long-term variance and μ represents the drift of the process for the stock.

Analogously as in the derivation of the original Black-Scholes equation we can justify the final form of the Heston pricing equation by the nonarbitrage argument. The main difference in its derivation is that one has to hedge away not only the risk associated with the change in the underlying (Δ) but also the risk stemming

2010 *Mathematics Subject Classification.* 35K10, 65N08, 65J10.
Key words and phrases. Tensor diffusion, diamond–cell, finite volumes, numerical solution.
This work was supported by the grant APVV-0184-10.

from the change of its variance (Υ). Using the concept of a well-hedged synthetic portfolio results into the following PDE for the unknown option price $V(S, v, t)$, cf. [14] :

$$\begin{aligned}\frac{\partial V}{\partial t} + rS\frac{\partial V}{\partial S} + \frac{1}{2}vS^2\frac{\partial^2 V}{\partial S^2} + \rho\sigma vS\frac{\partial^2 V}{\partial S \partial v} \\ + \frac{1}{2}\sigma^2 v\frac{\partial^2 V}{\partial v^2} + [\kappa(\theta - v) - \lambda v]\frac{\partial V}{\partial v} - rV = 0\end{aligned} \tag{3}$$

with λ representing the so-called market price of volatility risk and $r > 0$ the risk-free interest rate.

In order to complete the formulation of the problem let us define our domain of interest by $\ddot{\Omega} = (0, \infty) \times (0, \infty)$ and impose terminal and boundary conditions for a particular financial derivative. In this article we shall focus on the European call option which is a derivative giving the holder the right to purchase the underlying asset S for a predetermined strike price E at the expiration time T. The terminal condition for this derivative has the form

$$V(S, v, T) = \max(0, S - E). \tag{4}$$

The boundary conditions, due to Heston (cf. [12]), look as follows:

$$V(0, v, t) = 0, \tag{5}$$

$$\frac{\partial V}{\partial S}(S \to \infty, v, t) = 1, \tag{6}$$

$$\frac{\partial V}{\partial t}(S, 0, t) + rS\frac{\partial V}{\partial S}(S, 0, t) + \kappa\theta\frac{\partial V}{\partial v}(S, 0, t) - rV(S, 0, t) = 0, \tag{7}$$

$$V(S, v \to \infty, t) = S. \tag{8}$$

The boundary condition (5) for $S = 0$ follows from the stochastic differential equation (1). Particularly, if the price of the stock is zero, then the change of the stock price dS through time interval dt is zero. The second boundary condition (6) for $S \to \infty$ stems from the fact that if the stock price is very high in comparison with the strike price, one can almost neglect the effect of the strike price. On the boundary where $v = 0$ Heston imposes the hyperbolic equation (7) which can be derived directly from the governing equation (3) by inserting zero variance v. The last boundary condition (8) comes form the fact that option price can never exceed the price of the underlying.

Interestingly enough, note that although Heston imposes a Dirichlet boundary condition for $S = 0$ and a first-order hyperbolic equation on the boundary $v = 0$, we must take the so-called Fichera condition (cf. [8]) into account in order to judge whether it is necessary or not to specify these boundary conditions. The following Remark summarizes the main ideas, however the details may be found in Kútik's dissertation thesis, cf. [14].

Remark 1 (Fichera Conditions)**.** For the sake of further analysis let us write the equation (3) with the diffusion terms in the divergent form and accordingly adjusted velocity vector. We also revert the time by the transformation $\tau = T - t$ and obtain

$$\frac{\partial V}{\partial \tau} + \vec{\alpha} \cdot \nabla V - \nabla \cdot \tilde{\mathbf{B}} \nabla V + rV = 0 \tag{9}$$

where

$$\vec{\alpha} = -\begin{pmatrix} rS - vS - \frac{1}{2}\rho\sigma S \\ \kappa(\theta - v) - \lambda v - \frac{1}{2}\sigma^2 - \frac{1}{2}\rho\sigma v \end{pmatrix} \tag{10}$$

and

$$\tilde{\mathbf{B}} = \begin{pmatrix} \frac{1}{2}vS^2 & \frac{1}{2}\rho\sigma vS \\ \frac{1}{2}\rho\sigma vS & \frac{1}{2}\sigma^2 v \end{pmatrix}. \tag{11}$$

Denoting the unit outer normal vector relative to the domain boundary $\partial\ddot{\Omega}$ by $\vec{n}$, the Fichera conditions apply everywhere the vector $\tilde{\mathbf{B}}^T\vec{n}$ vanishes. Then, particularly for the parabolic Heston equation (3) the Fichera conditions read as follows: If for $S = 0$

$$\lim_{S\to 0} \vec{\alpha} \cdot \begin{pmatrix} -1 \\ 0 \end{pmatrix} \begin{cases} \geq 0 & \text{then } \mathbf{no} \text{ b.c. at } \quad S = 0 \quad \text{is needed,} \\ < 0 & \text{then b.c. at } \quad S = 0 \quad \text{is needed,} \end{cases} \tag{12}$$

in order to guarantee solution uniqueness. And if for $v = 0$

$$\lim_{v\to 0} \vec{\alpha} \cdot \begin{pmatrix} 0 \\ -1 \end{pmatrix} \begin{cases} \geq 0 & \text{then } \mathbf{no} \text{ b.c. at } \quad v = 0 \quad \text{is needed,} \\ < 0 & \text{then b.c. at } \quad v = 0 \quad \text{is needed,} \end{cases} \tag{13}$$

in order to guarantee solution uniqueness. Since (12) is always zero, no boundary condition is needed at $S = 0$. In the case of (13) we must not prescribe any boundary condition at $v = 0$ if $\kappa\theta - \frac{1}{2}\sigma^2 \geq 0$.

The purpose of this paper is to present a general finite volume discretization defined on a rectangular grid for the numerical solution of the described two-factor PDE vauation model. A finite volume discretization technique for the advection-diffusion-reaction PDEs of the type (3) has already been proposed by Zvan, Forsyth and Vetzal in [17]. In their approach they were however using a nonconservative discretization for this type of equation. Observing that the governing PDE (3) can be rewritten into a divergent form, the resulting conservative discretization by means of finite volume method becomes more natural in this context. Another justification for the finite volume approach is that the underlying PDE degenerates to a first-order hyperbolic equation on the boundary where $v = 0$. The finite volume discretization enables us to handle such cases, when there is no diffusion normal to the boundary, without any difficulties. And finally, if we intended to find a solution for some exotic options, which often requires a nonstandard computational domain, the finite volume method would support the use of unstructured triangular meshes, cf. [9].

One of the immediate questions, that arise after applying divergence theorem onto the the diffusion term, is associated with gradient approximation. In order to deal with this problem we use the so-called diamond-cell approximation which has already been applied in [6]. Moreover, error estimates and convergence rate have already been studied in the article of Coudiere, Vila and Villedieu, cf. [4].

Note that there are also other methods of solving the Heston PDE. Among others, the finite difference ADI schemes (cf. [13]) and Monte Carlo simulation methods (cf. [1]). In this paper, however we restrict ourselves to the study of the finite volume method.

An outline of the paper is as follows. Main focus of the second section is on the derivation of the numerical scheme. It consists of the discretization of the domain, implementation of the boundary conditions and the equation discretization. At the end of this section, we include a theoretical study of the existence and uniqueness of a solution to the corresponding system of linear equations. Then, we included a short section dealing with a numerical experiment showing that the scheme exhibits second order convergence in space. Finally, we conclude the paper and express our acknowledgments.

2. **Numerical Scheme.** Let us now deal with the application of the finite volume discretization method to the linear advection-diffusion-reaction equation (3) accompanied with the terminal condition (4) as well as a suitable discretized form of boundary conditions (5)-(8). In order to apply the finite volume discretization procedure, thus the Green's theorem, it is convenient to transform the governing equation (3) into a form with the diffusion term in divergent form, cf. [14] . In order to avoid variable coefficients in our scheme we introduce moreover a logarithmic transformation for the spatial variable $x = \ln\left(\frac{S}{E}\right)$. The other variables are $y = v$ and reverted time $\tau = T - t$. We can rewrite equation (3) in a matrix form for the unknown function $u(x, y, \tau) = V(S, v, t)/E$ as follows:

$$\frac{\partial u}{\partial \tau} + \vec{A} \cdot \nabla u = \nabla \cdot (\mathbf{B} \nabla u) - ru, \tag{14}$$

where

$$\mathbf{B} = \frac{1}{2} y \begin{pmatrix} 1 & \rho\sigma \\ \rho\sigma & \sigma^2 \end{pmatrix} \tag{15}$$

and

$$\vec{A} = -\begin{pmatrix} r - \frac{1}{2}y - \frac{1}{2}\rho\sigma \\ \kappa(\theta - y) - \lambda y - \frac{1}{2}\sigma^2 \end{pmatrix}. \tag{16}$$

Note that with the aforementioned transformation of variables the space-time domain $\ddot{\Omega}$ changed to $\dot{\Omega} = (-\infty, \infty) \times (0, \infty)$. Before constructing the numerical scheme for the PDE (14) this infinite domain has to be shrunk appropriately to $\Omega = (X_l, X_r) \times (0, Y)$ where X_l, X_r denote left and right bounds for the x-domain and Y denotes the upper bound of the y-domain. Furthermore, let p be a finite volume and σ_{pq} be an edge between p and q, $q \in N(p)$, where $N(p)$ is set of all neighbouring cells, i.e. finite volumes which have a common one-dimensional face with p. Let us define an admissible mesh $\mathcal{T}_h$ of the domain $\Omega \subset \mathbb{R}^2$, in the sense of [7], i.e. there exists a representative point $\mathbf{x}_p$ in the interior of every finite volume p such that the joining line between $\mathbf{x}_p$ and $\mathbf{x}_q$, $q \in N(p)$, is orthogonal to σ_{pq}. The discretization of Ω to $\mathcal{T}_h$ satisfies $\bar{\Omega} = \bigcup_{p \in \mathcal{T}_h} p$. Since we consider Ω to be a bounded rectangular domain, the admissible mesh $\mathcal{T}_h$ will consist of simple uniform rectangular finite volumes. Let $N_x, N_y \in \mathbb{N}$ and $h_x, h_y \in \mathbb{R}$ such that $h_x = (X_r - X_l)/N_x$ and $h_y = Y/N_y$ where h_x and h_y denote the uniform lengths of each rectangular finite volume in the x- and y-direction, respectively. Thus, in this case the measure of any finite volume p equals $m(p) = h_x\, h_y$. Now, let us define

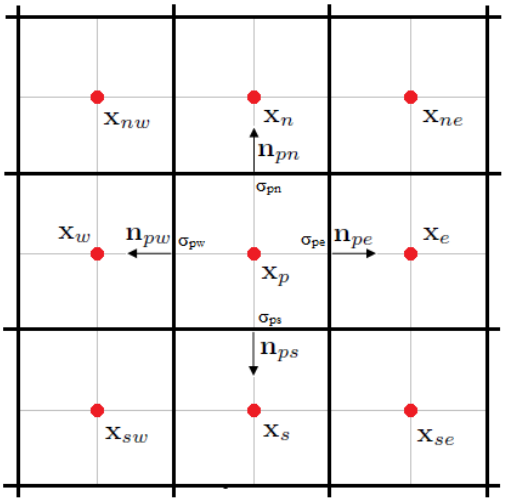

FIGURE 1. A detail of the finite volume mesh.

$$x_{\frac{1}{2}} = X_l, \;\; x_{i+\frac{1}{2}} = x_{i-\frac{1}{2}} + h_x, \;\; \text{for } i = 1, \ldots, N_x, \tag{17}$$

$$y_{\frac{1}{2}} = 0, \;\; y_{j+\frac{1}{2}} = y_{j-\frac{1}{2}} + h_y, \;\; \text{for } j = 1, \ldots, N_y. \tag{18}$$

Obviously, the upper bounds of each interval are defined as $x_{N_x+\frac{1}{2}} = X_r$ and $y_{N_y+\frac{1}{2}} = Y$. Then, the whole domain Ω is a union of $N_x \times N_y$ disjunct finite volumes

$$p_{ij} = (x_{i-\frac{1}{2}}, x_{i+\frac{1}{2}}) \times (y_{j-\frac{1}{2}}, y_{j+\frac{1}{2}}), \text{ for } i = 1, \dots, N_x \text{ and } j = 1, \dots, N_y. \tag{19}$$

Let us define the center of each finite volume p_{ij} by $\mathbf{x}_p = (x_i, y_j)$ as follows:

$$\begin{aligned} x_i &= x_{i-\frac{1}{2}} + \frac{h_x}{2}, \text{ for } i = 1, \dots, N_x, \\ y_j &= y_{j-\frac{1}{2}} + \frac{h_y}{2}, \text{ for } j = 1, \dots, N_y \end{aligned}$$

If we enlarge the set $N(p)$ by all finite volumes which have a common vertex with the cell p we obtain the set $N'(p)$. In the 2-dimensional case, $N'(p) = \{e, ne, n, nw, w, sw, s, se\}$ denotes east, north-east, north, north-west, west, south-west, south and south-east neighbouring cell of the finite volume p. Let the intersection point of σ_{pq} and line connecting $\mathbf{x}_p$ and $\mathbf{x}_q$, $q \in N(p)$ be denoted by $\mathbf{x}_{pq}$. We denote this orthonormal direction, i.e. the unit outer normal vector to σ_{pq} with respect to p, by $\vec{n}_{pq}$.

Concerning the time discretization, we use uniform discrete time step κ in order to discretize the time interval $[0, T]$. By introduction of the time stepping $\kappa = T/N_{ts}$ we can define the set of all discrete time layers $\tau^n = n\kappa$, $n = 0, 1, \dots, N_{ts}$ where N_{ts} denotes the number of all discrete time steps. Finally the constant numerical solution within a finite volume p at time step n is denoted by $u_p^n \approx u(\mathbf{x}_p, \tau^n)$.

2.1. **Boundary Conditions.** In order to obtain theoretical results and to perform numerical experiments we have to transform the terminal and boundary conditions to be consistent with the domain boundary $\partial\Omega$. Using the same transformations $x = \ln(\frac{S}{E}), y = v, \tau = T - t$ and $u(x, \tau) = \frac{V(S,t)}{E}$ as before we easily deduce that the terminal condition (4) for a European call option transforms to the following initial condition:

$$u(x, y, 0) = \max(e^x - 1, 0). \tag{20}$$

The first boundary condition (5) after transformation would be $u(-\infty, y, \tau) = 0$. Note that according to Remark 1 and (12), prescribing any boundary condition at $S = 0$ respectively at $x \to -\infty$ would be redundant. However, recall that we have approximated the infinite computational domain $\dot{\Omega}$ by a finite one, namely by $\Omega = (X_l, X_r) \times (0, Y)$. The Fichera condition derived in Remark 1 does not apply at $x = X_l$ and thus some artificial boundary condition must be prescribed. In our case it is natural to impose the original homogenous Dirichlet boundary condition:

$$u(X_l, y, \tau) = 0. \tag{21}$$

The case of the boundary condition at $S \to \infty$ respectively $x \to \infty$ must be treated similarly. Since we shrunk the domain $\dot{\Omega}$ to a finite domain Ω we should not neglect the substantial effect of the discounted strike price $Ee^{-r\tau}$. Hence the boundary term after transformation looks as follows:

$$u(X_r, y, \tau) = e^{X_r} - e^{-r\tau}. \tag{22}$$

Even though Heston imposes the boundary condition (7) at $v = 0$, one must follow the consequences of the Fichera condition. As we have written in Remark 1, in case when the condition $\kappa\theta - \frac{1}{2}\sigma^2 \geq 0$ holds—and we shall keep this restriction in the experimental part—there is no boundary condition needed for $v = 0$ and thus

for $y = 0$. Particularly, along the boundary $y = 0$, the equation (14) reduces to a hyperbolic PDE since the diffusion tensor (15) is zero here. The consequence is that the information on this boundary is transported only due to advection. And since the advection velocity vector (16) projected onto the unit outer normal vector is nonnegative only an outflow is realized at this point. In other words, no information can enter the domain from the region where $y < 0$.

In the numerical implementation part we extend the computational domain Ω to include a few additional so-called ghost cells $p_{i0} = (x_i, y_0),\ i = 1, \dots, N_x$ where $y_0 = -h_y/2$ (see [15]) and determine the ghost cell values $u^n_{p_{i0}},\ i = 1, \dots, N_x$ by extrapolation from the interior solution. The simplest approach is to take zero order extrapolation, meaning extrapolation by a constant function:

$$u^n_{p_{i0}} = u^n_{p_{i1}},\ i = 1, \dots, N_x. \tag{23}$$

The last condition $y \to \infty$ is also affected by shrinking of the interval $(0, \infty) \to (0, Y)$. We will not use the Dirichlet boundary condition (8) imposed by Heston since it would cause an unnatural jump in the solution. In order to implement our scheme for $y = Y$ we will simply assume that for a substantially large $y = \mathcal{O}(1)$, the solution is independent from y (see (8)). Hence, it is natural to impose artificial homogenous Neumann boundary conditions which can be implemented in the form of the constant extrapolation described above. By defining another set of ghost cells $p_{iN_y+1},\ i = 1, \dots, N_x$ with $y_{N_y+1} = y_{N_y} + h_y$, we can write

$$u^n_{p_{iN_y+1}} = u^n_{p_{iN_y}},\ i = 1, \dots, N_x. \tag{24}$$

Note that from a practical point of view, the hot-spot of the numerical solution is almost always very far away from the boundary conditions (22) and (24). Hence, they have only a little effect on the accuracy in the area of our interest.

2.2. **Equation Discretization.** Let us now discretize the governing equation (14) by the use of the so-called diamond-cell approximation, cf. [6, 4]. Although it has its diffusion term already in divergent form, inspired by [10], it is convenient to rewrite also the advection term into conservative and nonconservative part as follows:

$$\vec{A} \cdot \nabla u = \nabla \cdot (\vec{A}u) - (\nabla \cdot \vec{A})u. \tag{25}$$

Inserting this identity into (14), integrating it over a finite volume p and applying Green's theorem onto the terms $\nabla \cdot (\vec{A}u)$ and $\nabla \cdot (\mathbf{B}\nabla u)$ we obtain the following integral form:

$$\int_p \frac{\partial u}{\partial \tau} \mathrm{d}x + \sum_{q \in N(p)} \int_{\sigma_{pq}} \vec{A}u \cdot \vec{n}_{pq}\, \mathrm{d}\gamma - \int_p (\nabla \cdot \vec{A})u \mathrm{d}x = \sum_{q \in N(p)} \int_{\sigma_{pq}} \mathbf{B}\nabla u \cdot \vec{n}_{pq}\, \mathrm{d}\gamma - \int_p ru \mathrm{d}x. \tag{26}$$

Before we formulate the discretized version of (26), we shall have a look on the approximation of the vector $\mathbf{B}\nabla u$. To begin with, the diffusion tensor $\mathbf{B}$, can be expressed explicitly by

$$\mathbf{B} = \begin{pmatrix} b^{11} & b^{12} \\ b^{21} & b^{22} \end{pmatrix}$$

and then the diffusion tensor applied on the gradient of u is equal to

$$\mathbf{B}\nabla u = \begin{pmatrix} b^{11}\frac{\partial u}{\partial x} + b^{12}\frac{\partial u}{\partial y} \\ b^{21}\frac{\partial u}{\partial x} + b^{22}\frac{\partial u}{\partial y} \end{pmatrix}.$$

Let us denote by $\bar{u}_p$ a representative constant value of the solution in the cell p. By $\bar{u}_{pne}, \bar{u}_{pnw}, \bar{u}_{psw}, \bar{u}_{pse}$ we denote representative values in the north-east, north-west, south-west respectively south-east vertex of the finite volume p. Analogously, $\bar{u}_{pn}, \bar{u}_{pw}, \bar{u}_{ps}, \bar{u}_{pe}$ represents constant values on the north, west, south respectively east edge σ_{pq} of the finite volume p. We discretize the gradient on each edge σ_{pq} by using the diamond-cell approximation (see [6, p. 5]). The name of the approximation method comes from the diamond-like-shape of the area where the gradient is assumed to be constant. Following the terminology of Coudiere and Vila in [4] let us call these diamond-shaped areas co-volumes χ_σ. The co-volume χ_σ associated to σ is constructed by joining the endpoints of this edge and the midpoints $\mathbf{x}_p$ and $\mathbf{x}_q$ common to this edge (see Figure 2). Let us further denote the endpoints of an edge $\bar{\sigma} \subset \partial\chi_\sigma$ by $N_1(\bar{\sigma})$ and $N_2(\bar{\sigma})$. The unit normal vector to $\bar{\sigma}$ outward to χ_σ will be denoted by $\vec{n}_{\chi_\sigma,\bar{\sigma}}$. Now we are in shape to approximate the averaged gradient on χ_σ by

$$\frac{1}{m(\chi_\sigma)}\int_{\chi_\sigma} \nabla u \mathrm{d}x \approx \frac{1}{m(\chi_\sigma)}\sum_{\bar{\sigma}\subset\partial\chi_\sigma} \frac{\bar{u}_{N_1(\bar{\sigma})} + \bar{u}_{N_2(\bar{\sigma})}}{2} m(\bar{\sigma})\vec{n}_{\chi_\sigma,\bar{\sigma}}$$

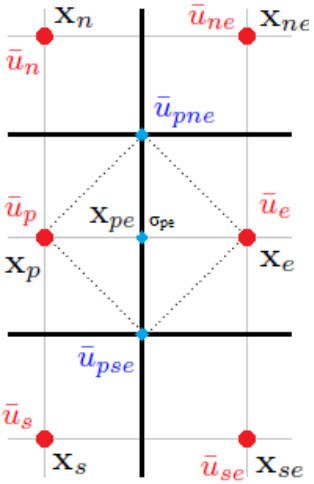

FIGURE 2. A detail of the diamond-cell approximation of the gradient on the edge σ_{pe} .

Since our mesh is rectangular, we can use the following relations: $m(\chi_\sigma) = h_x h_y/2$ and $m(\bar{\sigma}) = \frac{\sqrt{h_x^2+h_y^2}}{2}$. For the sake of brief notation we will use the symbol $\nabla_{pq}^{DC} = (\nabla_{pq,x}^{DC}, \nabla_{pq,y}^{DC})$ when using the diamond-cell gradient operator on the edge σ_{pq}. If we calculate the gradient approximation on the edge σ_{pe} we end up with

$$\nabla_{pe}^{DC} u = \frac{1}{m(\chi_{\sigma_{pe}})}\sum_{\bar{\sigma}\subset\partial\chi_{\sigma_{pe}}} \frac{\bar{u}_{N_1(\bar{\sigma})} + \bar{u}_{N_2(\bar{\sigma})}}{2} m(\bar{\sigma})\vec{n}_{\chi_{\sigma_{pe}},\bar{\sigma}} = \begin{pmatrix} \frac{\bar{u}_e - \bar{u}_p}{h_x} \\ \frac{\bar{u}_{pne} - \bar{u}_{pse}}{h_y} \end{pmatrix} \quad (27)$$

and for the remaining edges σ_{pw}, σ_{pn} and σ_{ps} we can write

$$\nabla_{pw}^{DC} u = \begin{pmatrix} \frac{\bar{u}_p - \bar{u}_w}{h_x} \\ \frac{\bar{u}_{pnw} - \bar{u}_{psw}}{h_y} \end{pmatrix}, \quad \nabla_{pn}^{DC} u = \begin{pmatrix} \frac{\bar{u}_{pne} - \bar{u}_{pnw}}{h_x} \\ \frac{\bar{u}_n - \bar{u}_p}{h_y} \end{pmatrix}, \quad \nabla_{ps}^{DC} u = \begin{pmatrix} \frac{\bar{u}_{pse} - \bar{u}_{psw}}{h_x} \\ \frac{\bar{u}_p - \bar{u}_s}{h_y} \end{pmatrix}. \quad (28)$$

Replacing the exact gradient with its diamond-cell approximation we can approximate the exact averaged diffusion flux on the edge σ_{pq} by

$$\frac{1}{m(\sigma_{pq})}\int_{\sigma_{pq}} \mathbf{B}\nabla u \cdot \vec{n}_{pq}\, \mathrm{d}\gamma \approx \mathbf{B}_{pq}\nabla_{pq}^{DC} u \cdot \vec{n}_{pq} \quad (29)$$

with $\mathbf{B}_{pq}$ defined as the averaged diffusion tensor along the edge σ_{pq}.

Regarding both terms associated with the advection, assuming a constant solution in each finite volume we can use the following approximations

$$\int_{\sigma_{pq}} \vec{A}u \cdot \vec{n}_{pq}\,\mathrm{d}\gamma \approx \bar{u}_{pq} v_{pq} m(\sigma_{pq}),\ \int_p (\nabla \cdot \vec{A}) u \mathrm{d}x \approx \bar{u}_p v_{pq} m(\sigma_{pq}) \tag{30}$$

where v_{pq} denotes the exact averaged advection velocity on the face σ_{pq} in the inward normal direction to the finite volume p, i.e.

$$v_{pq} = -\frac{1}{m(\sigma_{pq})} \int_{\sigma_{pq}} \vec{A} \cdot \vec{n}_{pq}\,\mathrm{d}\gamma. \tag{31}$$

Denoting the averaged advection vector $\vec{A}$ along the edge σ_{pq} by $\vec{A}_{pq}$ we can formulate v_{pq}, by $v_{pq} = -\vec{A}_{pq} \cdot \vec{n}_{pq}$. Particularly, for each edge σ_{pq}, the velocity v_{pq} can be written as

$$v_{pn} = -a^2_{pn},\ v_{pw} = a^1_{pw},\ v_{pe} = -a^1_{pe},\ v_{ps} = a^2_{ps} \tag{32}$$

where a^1_{pq}, a^2_{pq} are the mean values of the components of the advection velocity vector $\vec{A} = \left(a^1, a^2\right)^T$ evaluated along the edge σ_{pq}. Plugging approximations (30) as well as the definitions of the numerical diffusion flux and advection velocity into (26) and assuming constant solution in the source term we get

$$\begin{aligned}\int_p \frac{\partial u}{\partial \tau}\mathrm{d}x + \sum_{q \in N(p)} (-\vec{A}_{pq} \cdot \vec{n}_{pq})\,(\bar{u}_p - \bar{u}_{pq})\, m(\sigma_{pq}) = \\ \sum_{q \in N(p)} \mathbf{B}_{pq} \nabla^{DC}_{pq} u \cdot \vec{n}_{pq} m(\sigma_{pq}) - r \bar{u}_p m(p).\end{aligned} \tag{33}$$

After expanding the advection and diffusion terms in (33) we get

$$\begin{aligned}&\int_p \frac{\partial u}{\partial \tau}\mathrm{d}x + r\,\bar{u}_p\, m(p) \\ &- m(\sigma_{pe}) a^1_{pe} (\bar{u}_p - \bar{u}_{pe}) - m(\sigma_{pe}) \left[b^{11}_{pe} \frac{\bar{u}_e - \bar{u}_p}{h_x} + b^{12}_{pe} \frac{\bar{u}_{pne} - \bar{u}_{pse}}{h_y} \right] \\ &- m(\sigma_{pn}) a^2_{pn} (\bar{u}_p - \bar{u}_{pn}) - m(\sigma_{pn}) \left[b^{21}_{pn} \frac{\bar{u}_{pne} - \bar{u}_{pnw}}{h_x} + b^{22}_{pn} \frac{\bar{u}_n - \bar{u}_p}{h_y} \right] \\ &+ m(\sigma_{pw}) a^1_{pw} (\bar{u}_p - \bar{u}_{pw}) + m(\sigma_{pw}) \left[-b^{11}_{pw} \frac{\bar{u}_w - \bar{u}_p}{h_x} - b^{12}_{pw} \frac{\bar{u}_{psw} - \bar{u}_{pnw}}{h_y} \right] \\ &+ m(\sigma_{ps}) a^2_{ps} (\bar{u}_p - \bar{u}_{ps}) + m(\sigma_{ps}) \left[-b^{21}_{ps} \frac{\bar{u}_{psw} - \bar{u}_{pse}}{h_x} - b^{22}_{ps} \frac{\bar{u}_s - \bar{u}_p}{h_y} \right] = 0.\end{aligned} \tag{34}$$

In order to formulate the following numerical scheme we need to replace the representative values of the solution $\bar{u}^m_p$ and $\bar{u}^m_{pq}$, $m = n-1$, n by a combination of the numerical solution in the grid points. The most natural choice for reconstructions $\bar{u}^m_p$ and $\bar{u}^m_{pq}$ is given by

$$\bar{u}^m_p = u^m_p, \qquad \bar{u}^m_{pq} = \frac{u^m_p + u^m_q}{2},\ \text{if } q \in N(p), \tag{35}$$

$$\bar{u}^m_{pne} = \frac{u^m_p + u^m_e + u^m_{ne} + u^m_n}{4}, \quad \bar{u}^m_{pnw} = \frac{u^m_p + u^m_n + u^m_{nw} + u^m_w}{4}, \tag{36}$$

$$\bar{u}^m_{psw} = \frac{u^m_p + u^m_w + u^m_{sw} + u^m_s}{4}, \quad \bar{u}^m_{pse} = \frac{u^m_p + u^m_s + u^m_{se} + u^m_e}{4}. \tag{37}$$

Inserting (35)-(37) into (34) with $m = n$ and replacing the time derivative $\frac{\partial u}{\partial \tau}$ by the backward difference $\frac{u^n - u^{n-1}}{\kappa}$ we obtain the diamond-cell fully-implicit scheme in the form

$$(1 + \kappa r)u_p^n + \frac{\kappa}{m(p)} \sum_{q \in N'(p)} c_{pq} \left(u_p^n - u_q^n\right) = u_p^{n-1} \tag{38}$$

where in order to simplify the notation of the scheme we have introduced new coefficients

$$\begin{aligned} c_{pq} &= a_{pq} + b_{pq}, \quad && q \in N(p), \\ c_{pq} &= b_{pq}, && q \in N'(p) \backslash N(p). \end{aligned}$$

with $a_{pq}, q \in N(p)$ and $b_{pq}, q \in N'(p)$ which we define as follows

$$a_{pe} = -\frac{1}{2} h_y a_{pe}^1, \; a_{pw} = \frac{1}{2} h_y a_{pw}^1, \; a_{pn} = -\frac{1}{2} h_x a_{pn}^2, \; a_{ps} = \frac{1}{2} h_x a_{ps}^2, \tag{39}$$

$$b_{pe} = \frac{h_y}{h_x} b_{pe}^{11} + \frac{b_{pn}^{21}}{4} - \frac{b_{ps}^{21}}{4}, \; b_{pw} = \frac{h_y}{h_x} b_{pw}^{11} - \frac{b_{pn}^{21}}{4} + \frac{b_{ps}^{21}}{4}, \tag{40}$$

$$b_{pn} = \frac{h_x}{h_y} b_{pn}^{22} + \frac{b_{pe}^{12}}{4} - \frac{b_{pw}^{12}}{4}, \; b_{ps} = \frac{h_x}{h_y} b_{ps}^{22} - \frac{b_{pe}^{12}}{4} + \frac{b_{pw}^{12}}{4}, \tag{41}$$

$$b_{pne} = \frac{b_{pe}^{12}}{4} + \frac{b_{pn}^{21}}{4}, \; b_{psw} = \frac{b_{pw}^{12}}{4} + \frac{b_{ps}^{21}}{4}, \; b_{pnw} = -\frac{b_{pw}^{12}}{4} - \frac{b_{pn}^{21}}{4}, \; b_{pse} = -\frac{b_{pe}^{12}}{4} - \frac{b_{ps}^{21}}{4}. \tag{42}$$

2.3. **Theoretical Properties.** In this subsection our goal is to study the existence and uniqueness of the numerical solution generated by the diamond–cell scheme (38). In the proof we mainly follow the ideas in the article [4] by Coudiere and Vila and the article [6] by Drblíková and Mikula. It is important to note that when talking about the diffusion tensor $\mathbf{B}$ or the advection vector $\vec{A}$ we have so far always written them in the standard basis $(\varepsilon_1, \varepsilon_2)$ (cf. (27), (28) and (32)). In order to simplify further analysis, although it may look artificial, we will also consider both $\mathbf{B}$ and $\vec{A}$ in the local basis $(\vec{n}_{W,\sigma}, \vec{t}_{W,\sigma})$, cf. [4]. Note that in this case we label "north", "south", "west" and "east" by capital letters N, S, W and E to emphasize that the points are treated in the local basis relative to the edge σ. The couple $(\vec{n}_{W,\sigma}, \vec{t}_{W,\sigma})$ denotes a unit normal vector relative to the edge σ outward to W and a unit vector parallel to σ, respectively, such that $(\mathbf{x}_N - \mathbf{x}_S) \cdot \vec{t}_{W,\sigma} > 0$. Moreover, $\sigma = \sigma_{WE}$ always represents the edge between cells W and E in the local basis. Symbols $\mathbf{x}_N$ and $\mathbf{x}_S$ denote the northern and southern vertex of the edge σ (cf. Figure 3 and 4). Similarly, by $\mathbf{x}_W$ and $\mathbf{x}_E$ we label west and east neighbouring cell centers. Symbols d_{EW} and d_{NS} denote the distance $|\mathbf{x}_E - \mathbf{x}_W|$ and $|\mathbf{x}_N - \mathbf{x}_S|$, respectively. In our setting this is

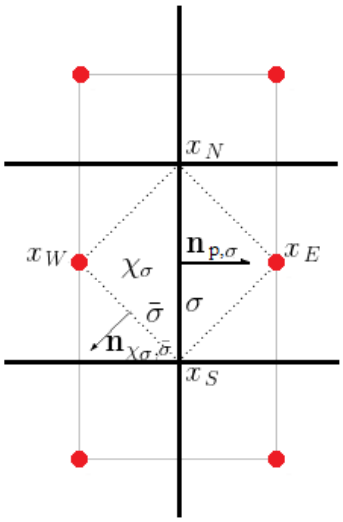

FIGURE 3. A detail of the diamond-cell approximation of the gradient on the edge σ written in the local basis: points $\mathbf{x}_N$, $\mathbf{x}_S$ denote the northern and southern vertex of the edge σ and $\mathbf{x}_W$, $\mathbf{x}_E$ denote the western and eastern cell centers associated to the edge σ.

equal either to h_x or h_y depending on the position of the edge σ. Values $\bar{u}_E$, $\bar{u}_W$, $\bar{u}_N$ and $\bar{u}_S$ can be reconstructed analogically to (35)-(37). In the case of the scheme (38) we take all numerical values u from the new time layer τ^n. Taking into account the notation of the north, west, east and south edge by σ_{pn}, σ_{pw}, σ_{pe} and σ_{ps} relative to the finite volume p (cf. Figure 1) the labeling of neighbours in the local basis for corresponding edges illustrated in Figure 4 becomes clearer. Note that the cell W in local basis notation always coincides with the cell p written in the standard basis.

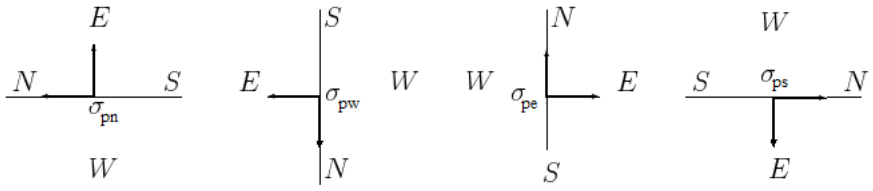

FIGURE 4. The notation for corresponding edges σ_{pn}, σ_{pw}, σ_{pe} and σ_{ps}. The perpendicular vector is the unit outer normal vector $\vec{n}_{W,\sigma}$ and the parallel one is the unit tangent vector $\vec{t}_{W,\sigma}$.

Let us further denote by ε_p the set of edges such that $\partial p = \bigcup_{\sigma\in\varepsilon_p}\sigma$. Let ε_{int} denote the set of all interior edges. Moreover, we can also define ε_{ext} as the set of all boundary edges, i.e. $\varepsilon_{\text{ext}} = \varepsilon \cap \partial\Omega$ where ε is the set of all edges from the admissible mesh $\mathcal{T}_h$, i.e. $\varepsilon = \bigcup_{p\in\mathcal{T}_h}\varepsilon_p$. The set ε_{ext} can be further decomposed into two subsets $\varepsilon_{\text{ext}} = \varepsilon_{\text{ext}}^{\text{DBC}} \cup \varepsilon_{\text{ext}}^{\text{GCE}}$ with $\varepsilon_{\text{ext}}^{\text{DBC}}$ denoting all exterior boundary edges where Dirichlet boundary conditions are prescribed and $\varepsilon_{\text{ext}}^{\text{GCE}}$ denoting all boundary edges where the ghost cell extrapolation applies. In our setting $\varepsilon_{\text{ext}}^{\text{DBC}}$ corresponds to the boundary condition (21) for $x = X_l$ and (22) for $x = X_r$. Similarly, in the implementation part of the European call option $\varepsilon_{\text{ext}}^{\text{GCE}}$ is effectively the boundary (23) for $y = 0$ and (24) for $y = Y$.

Having introduced such alternative notation we are in shape to rewrite the diamond-cell approximation of the gradient (27) along any edge σ as follows:

$$\nabla_\sigma^{DC} u = \frac{u_E - u_W}{d_{EW}}\vec{n}_{W,\sigma} + \frac{u_N - u_S}{d_{NS}}\vec{t}_{W,\sigma} \tag{43}$$

Let us further define the discrete numerical solution by

$$u_{h,k}(\mathbf{x},\tau) = \sum_{n=0}^{N_{ts}}\sum_{p\in\mathcal{T}_h} u_p^n \chi_{\{x\in p\}}\chi_{\{\tau^{n-1}<\tau\le\tau^n\}} \tag{44}$$

where the function $\chi_{\{A\}}$ is defined as

$$\chi_{\{A\}} = \begin{cases} 1, & \text{if A is true,} \\ 0, & \text{elsewhere} \end{cases} \tag{45}$$

and let $u_{h,k}^n(\mathbf{x},\tau) = \sum_{p\in\mathcal{T}_h} u_p^n \chi_{\{x\in p\}}$ denote a finite volume approximation at the n^{th} time step. Then, in order to get the scheme written in terms of the local basis let us denote by Φ_σ^n the approximation of the exact averaged diffusion flux

$$\Phi_\sigma^n(u_{h,k}^n) \approx \frac{1}{m(\sigma)}\int_\sigma \mathbf{B}\nabla u^n \cdot \vec{n}_{W,\sigma}\mathrm{d}\gamma \tag{46}$$

for any $\sigma \in \varepsilon$. Replacing the exact gradient ∇u by its diamond-cell approximation (43) we can write the numerical diffusion flux as

$$\Phi_\sigma^n(u_{h,\mathcal{K}}^n) = (\mathbf{B}_\sigma \nabla_\sigma^{DC} u^n) \cdot \vec{n}_{W,\sigma} \tag{47}$$

where

$$\mathbf{B}_\sigma = \begin{pmatrix} \bar{b}_\sigma^{11} & \bar{b}_\sigma^{12} \\ \bar{b}_\sigma^{21} & \bar{b}_\sigma^{22} \end{pmatrix} \tag{48}$$

is the mean value of the tensor $\mathbf{B}$ along the edge σ. It is important to note that the diffusion tensor (48) is also written in the basis $(\vec{n}_{W,\sigma}, \vec{t}_{W,\sigma})$ and the coefficients $\bar{b}_\sigma^{ij}$ need to be determined accordingly. Since the formula (43) can be written as

$$\nabla_\sigma^{DC} u^n = \begin{pmatrix} \frac{u_E^n - u_W^n}{d_{EW}} \\ \frac{u_N^n - u_S^n}{d_{NS}} \end{pmatrix} \tag{49}$$

and $\vec{n}_{W,\sigma} = (1,0)^T$, both in the local basis notation, we can formulate (47) equivalently as follows:

$$\Phi_\sigma^n(u_{h,\mathcal{K}}^n) = \left[\begin{pmatrix} \bar{b}_\sigma^{11} & \bar{b}_\sigma^{12} \\ \bar{b}_\sigma^{21} & \bar{b}_\sigma^{22} \end{pmatrix} \begin{pmatrix} \frac{u_E^n - u_W^n}{d_{EW}} \\ \frac{u_N^n - u_S^n}{d_{NS}} \end{pmatrix} \right] \cdot \begin{pmatrix} 1 \\ 0 \end{pmatrix} = \bar{b}_\sigma^{11} \frac{u_E^n - u_W^n}{d_{EW}} + \bar{b}_\sigma^{12} \frac{u_N^n - u_S^n}{d_{NS}}. \tag{50}$$

In order to obtain the values $\bar{b}^{11}$ and $\bar{b}^{12}$ let us write the numerical diffusion flux for each edge in the standard basis and then compare with (50):

$$\Phi_{\sigma_{pn}}^n = \left[\begin{pmatrix} b_{pn}^{11} & b_{pn}^{12} \\ b_{pn}^{21} & b_{pn}^{22} \end{pmatrix} \begin{pmatrix} \frac{u_S^n - u_N^n}{d_{NS}} \\ \frac{u_E^n - u_W^n}{d_{EW}} \end{pmatrix} \right] \cdot \begin{pmatrix} 0 \\ 1 \end{pmatrix} = b_{pn}^{22} \frac{u_E^n - u_W^n}{d_{EW}} - b_{pn}^{21} \frac{u_N^n - u_S^n}{d_{NS}},$$

$$\Phi_{\sigma_{pw}}^n = \left[\begin{pmatrix} b_{pw}^{11} & b_{pw}^{12} \\ b_{pw}^{21} & b_{pw}^{22} \end{pmatrix} \begin{pmatrix} \frac{u_W^n - u_E^n}{d_{EW}} \\ \frac{u_S^n - u_N^n}{d_{NS}} \end{pmatrix} \right] \cdot \begin{pmatrix} -1 \\ 0 \end{pmatrix} = b_{pw}^{11} \frac{u_E^n - u_W^n}{d_{EW}} + b_{pw}^{12} \frac{u_N^n - u_S^n}{d_{NS}},$$

$$\Phi_{\sigma_{pe}}^n = \left[\begin{pmatrix} b_{pe}^{11} & b_{pe}^{12} \\ b_{pe}^{21} & b_{pe}^{22} \end{pmatrix} \begin{pmatrix} \frac{u_E^n - u_W^n}{d_{EW}} \\ \frac{u_N^n - u_S^n}{d_{NS}} \end{pmatrix} \right] \cdot \begin{pmatrix} 1 \\ 0 \end{pmatrix} = b_{pe}^{11} \frac{u_E^n - u_W^n}{d_{EW}} + b_{pe}^{12} \frac{u_N^n - u_S^n}{d_{NS}},$$

$$\Phi_{\sigma_{ps}}^n = \left[\begin{pmatrix} b_{ps}^{11} & b_{ps}^{12} \\ b_{ps}^{21} & b_{ps}^{22} \end{pmatrix} \begin{pmatrix} \frac{u_N^n - u_S^n}{d_{NS}} \\ \frac{u_W^n - u_E^n}{d_{EW}} \end{pmatrix} \right] \cdot \begin{pmatrix} 0 \\ -1 \end{pmatrix} = b_{ps}^{22} \frac{u_E^n - u_W^n}{d_{EW}} - b_{ps}^{21} \frac{u_N^n - u_S^n}{d_{NS}}.$$

Clearly, $\bar{b}_\sigma^{11} = b_\sigma^{11}$, $\bar{b}_\sigma^{12} = b_\sigma^{12}$ for the two edges $\sigma = \sigma_{pw}$, $\sigma = \sigma_{pe}$ and $\bar{b}_\sigma^{11} = b_\sigma^{22}$, $\bar{b}_\sigma^{12} = -b_\sigma^{21}$ for the two edges $\sigma = \sigma_{pn}$, $\sigma = \sigma_{ps}$.

In order to continue with the analysis it is convenient to transform the averaged exact advection velocity approximation (31) into the local basis as well. Recall that in our scheme we approximate terms associated with the advection in the standard basis by

$$\int_{\sigma_{pq}} \vec{A}u \cdot \vec{n}_{pq} \, \mathrm{d}\gamma - \int_p (\nabla \cdot \vec{A}) u \mathrm{d}x \approx \int_{\sigma_{pq}} \vec{A} \cdot \vec{n}_{pq} \mathrm{d}\gamma (\bar{u}_{pq} - \bar{u}_p). \tag{51}$$

Let us denote the approximation of the averaged advection-associated flux term appearing on the right-hand side of (51) written in the local basis by $\Psi_\sigma^n(u_{h,\mathcal{K}}^n)$, i.e.

$$\Psi_\sigma^n(u_{h,\mathcal{K}}^n) \approx \frac{1}{m(\sigma)} \int_\sigma \vec{A} \cdot \vec{n}_{W,\sigma} \mathrm{d}\gamma (\bar{u}_{EW}^n - \bar{u}_W^n) \tag{52}$$

Denoting by $\vec{A}_\sigma$ the approximation of the mean value of the vector $\vec{A}$ along the edge σ in the local basis and applying the reconstruction $\bar{u}_{WE} = (u_W + u_E)/2$ we

can define $\Psi_\sigma^n(u_{h,\mathcal{k}}^n)$ as follows

$$\Psi_\sigma^n(u_{h,\mathcal{k}}^n) = (\vec{A}_\sigma \cdot \vec{n}_{W,\sigma})\frac{u_E^n - u_W^n}{2}. \tag{53}$$

Furthermore, since $\vec{A}_\sigma \cdot \vec{n}_{W,\sigma} = (\bar{a}_\sigma^1, \bar{a}_\sigma^2)(1,0)^T = \bar{a}_\sigma^1$ we can rewrite (53) more simply as

$$\Psi_\sigma^n(u_{h,\mathcal{k}}^n) = \bar{a}_\sigma^1\frac{u_E^n - u_W^n}{2}. \tag{54}$$

It remains to determine the form of the coefficients $\bar{a}_\sigma^1$. To do so, let us write the numerical advection flux on each edge in the standard basis:

$$\begin{aligned}
\Psi_{\sigma_{pn}}^n &= \begin{pmatrix} a_{pn}^1 \\ a_{pn}^2 \end{pmatrix} \cdot \begin{pmatrix} 0 \\ 1 \end{pmatrix} \frac{u_E^n - u_W^n}{2} = a_{pn}^2 \frac{u_E^n - u_W^n}{2}, \\
\Psi_{\sigma_{pw}}^n &= \begin{pmatrix} a_{pw}^1 \\ a_{pw}^2 \end{pmatrix} \cdot \begin{pmatrix} -1 \\ 0 \end{pmatrix} \frac{u_E^n - u_W^n}{2} = -a_{pw}^1 \frac{u_E^n - u_W^n}{2}, \\
\Psi_{\sigma_{pe}}^n &= \begin{pmatrix} a_{pe}^1 \\ a_{pe}^2 \end{pmatrix} \cdot \begin{pmatrix} 1 \\ 0 \end{pmatrix} \frac{u_E^n - u_W^n}{2} = a_{pe}^1 \frac{u_E^n - u_W^n}{2}, \\
\Psi_{\sigma_{ps}}^n &= \begin{pmatrix} a_{ps}^1 \\ a_{ps}^2 \end{pmatrix} \cdot \begin{pmatrix} 0 \\ -1 \end{pmatrix} \frac{u_E^n - u_W^n}{2} = -a_{ps}^2 \frac{u_E^n - u_W^n}{2}.
\end{aligned}$$

The comparison with (54) yields $\bar{a}_\sigma^1 = a_\sigma^2$ for the edge $\sigma = \sigma_{pn}$, $\bar{a}_\sigma^1 = -a_\sigma^1$ for the edge $\sigma = \sigma_{pw}$, $\bar{a}_\sigma^1 = a_\sigma^1$ for the edge $\sigma = \sigma_{pe}$ and $\bar{a}_\sigma^1 = -a_\sigma^2$ for the edge $\sigma = \sigma_{ps}$.

Using definitions (50) and (53) we can summarize our fully-implicit scheme written in terms of the local basis $(\vec{n}_{W,\sigma}, \vec{t}_{W,\sigma})$:

$$\frac{u_W^n - u_W^{n-1}}{\mathcal{k}} m(W) - \sum_{\sigma\in\varepsilon_W} \Phi_\sigma^n(u_{h,\mathcal{k}}^n)m(\sigma) + \sum_{\sigma\in\varepsilon_W} \Psi_\sigma^n(u_{h,\mathcal{k}}^n)m(\sigma) + r u_W^n m(W) = 0. \tag{55}$$

Let us now introduce a space of piecewise constant functions associated to our mesh and a discrete H^1 seminorm for this space. This seminorm will be used to obtain some estimates on numerical solution generated by the scheme (38).

Definition 2.1. Let Ω be an open bounded polygonal subset of $\mathbb{R}^2$. Let $\mathcal{T}_h$ be an admissible finite volume mesh in the sense of [7]. We define $\mathcal{P}_0(\mathcal{T}_h)$ as the set of functions from Ω to $\mathbb{R}$ which are constant over each finite volume p of the mesh $\mathcal{T}_h$.

Definition 2.2. Let Ω be an open bounded polygonal subset of $\mathbb{R}^2$. For $u_{h,\mathcal{k}}^n \in \mathcal{P}_0(\mathcal{T}_h)$ we define

$$|u_{h,\mathcal{k}}^n|_{1,\mathcal{T}_h} = \left(\sum_{\sigma\in\varepsilon_{\text{int}}} \frac{(u_E^n - u_W^n)^2}{d_{EW}} m(\sigma) \right)^{\frac{1}{2}}. \tag{56}$$

where d_{EW} denotes the Euclidean distance between $\mathbf{x}_E$ and $\mathbf{x}_W$ and $m(\sigma) = d_{NS}$.

Having our scheme written in the local basis notation (55), we can proceed with a theorem stating that a unique solution to the corresponding system of linear equations does exist. In order to formulate proper existence and uniqueness conditions let us first expand the diffusion and advection term appearing in (55) on the boundary edges $\sigma \in \varepsilon_{\text{ext}}$ and separate all boundary terms. Noting that both Dirichlet boundary conditions (21) and (22) are constant, the term $u_N^n - u_S^n = 0$, $\forall\sigma \in \varepsilon_{\text{ext}}^{\text{DBC}}$. Furthermore, since we are using constant extrapolation of the solution to the ghost

cells, $u_E^n - u_W^n = 0,\ \forall \sigma \in \varepsilon_{\text{ext}}^{\text{GCE}}$. Taking these identities into account we can expand the expression $\Phi_\sigma^n(u_{h,\mathcal{k}}^n),\ \forall \sigma \in \varepsilon_{\text{ext}}$ as follows:

$$\begin{aligned}\Phi_\sigma^n(u_{h,\mathcal{k}}^n) = \Phi_\sigma^n(u_{h,\mathcal{k}}^n)\chi_{\{\sigma\in\varepsilon_{\text{ext}}^{\text{DBC}}\}} + \Phi_\sigma^n(u_{h,\mathcal{k}}^n)\chi_{\{\sigma\in\varepsilon_{\text{ext}}^{\text{GCE}}\}} = \\ \bar{b}_\sigma^{11}\frac{u_\sigma^n - u_W^n}{d_{W\sigma}}\chi_{\{\sigma\in\varepsilon_{\text{ext}}^{\text{DBC}}\}} + \bar{b}_\sigma^{12}\frac{u_N^n - u_S^n}{d_{NS}}\chi_{\{\sigma\in\varepsilon_{\text{ext}}^{\text{GCE}}\}}\end{aligned} \tag{57}$$

where in the first term, evaluated on $\sigma \in \varepsilon_{\text{ext}}^{\text{DBC}}$, we have replaced u_E^n by the prescribed Dirichlet boundary condition, i.e. $u_E^n = u_\sigma^n$ and d_{EW} by the Euclidean distance between the point $\mathbf{x}_W$ and the representative point $\mathbf{x}_{\sigma_{EW}}$, i.e. $d_{EW} = d_{W\sigma}$. For the sake of simplicity, henceforth we will denote the edges where Dirichlet boundary conditions apply by σ and those neighbouring with the ghost cells by σ_{GC}. Note that the term $u_N^n - u_S^n$ also contains Dirichlet boundary condition if it is evaluated in the corner cells of the domain Ω. Let us denote these corner cells in the following by $ne = p_{N_x,N_y}$, $nw = p_{1,N_y}$, $sw = p_{1,1}$ and $se = p_{N_x,1}$. Let us denote by $\varepsilon_{\text{cor}}^{\text{GCE}}$ the subset of $\varepsilon_{\text{ext}}^{\text{GCE}}$ consisting only of the four ghost-cell-edges positioned in the corner cells.

Similarly to the boundary diffusion fluxes let us now expand advection fluxes on $\sigma \in \varepsilon_{\text{ext}}$ as well. Since $u_E^n - u_W^n = 0,\ \forall \sigma \in \varepsilon_{\text{ext}}^{\text{GCE}}$ we can rewrite the expression $\Psi_\sigma^n(u_{h,\mathcal{k}}^n),\ \forall \sigma \in \varepsilon_{\text{ext}}$ as follows:

$$\Psi_\sigma^n(u_{h,\mathcal{k}}^n) = \bar{a}_\sigma^1\frac{u_\sigma^n - u_W^n}{2}\chi_{\{\sigma\in\varepsilon_{\text{ext}}^{\text{DBC}}\}} \tag{58}$$

Let us now define a discrete operator $\mathcal{L}_h$ with respect to the form of (55), (57) and (58) by

$$\begin{aligned}\mathcal{L}_h(u_{h,\mathcal{k}}^n) =& u_W^n m(W) - \mathcal{k}\sum_{\sigma\in\varepsilon_W\cap\varepsilon_{\text{int}}}\Phi_\sigma^n(u_{h,\mathcal{k}}^n)m(\sigma) \\ &+ \mathcal{k}\frac{\bar{b}_\sigma^{11}}{d_{W\sigma}}u_W^n\chi_{\{\sigma\in\varepsilon_W\cap\varepsilon_{\text{ext}}^{\text{DBC}}\}}m(\sigma) \\ &+ \mathcal{k}\bar{b}_\sigma^{12}\left(u_N^n - u_S^n\right)\chi_{\{\sigma\in\varepsilon_W\cap\left(\varepsilon_{\text{ext}}^{\text{GCE}}\setminus\varepsilon_{\text{cor}}^{\text{GCE}}\right)\}} \\ &+ \mathcal{k}\big(\bar{b}_{\sigma_{GC}}^{12}u_N^n\chi_{\{W=ne\}} - \bar{b}_{\sigma_{GC}}^{12}u_S^n\chi_{\{W=nw\}} \\ &\quad + \bar{b}_{\sigma_{GC}}^{12}u_N^n\chi_{\{W=sw\}} - \bar{b}_{\sigma_{GC}}^{12}u_S^n\chi_{\{W=se\}}\big) \\ &+ \mathcal{k}\sum_{\sigma\in\varepsilon_W\cap\varepsilon_{\text{int}}}\Psi_\sigma^n(u_{h,\mathcal{k}}^n)m(\sigma) - \mathcal{k}\frac{\bar{a}_\sigma^1}{2}u_W^n\chi_{\{\sigma\in\varepsilon_W\cap\varepsilon_{\text{ext}}^{\text{DBC}}\}}m(\sigma) \\ &+ r\mathcal{k}u_W^n m(W).\end{aligned} \tag{59}$$

Hence the numerical solution $u_{h,\mathcal{k}}^n \in \mathcal{P}_0(\mathcal{T}_h)$ of the scheme (55) is given by

$$\mathcal{L}_h(u_{h,\mathcal{k}}^n) = f_{h,\mathcal{k}}(u_{h,\mathcal{k}}^{n-1}) \tag{60}$$

with the right-hand side function $f_{h,\mathcal{k}}(u_{h,\mathcal{k}}^{n-1})$ defined as

$$\begin{aligned}f_{h,\mathcal{k}}(u_{h,\mathcal{k}}^{n-1}) =& u_W^{n-1}m(W) + \mathcal{k}\left(\frac{\bar{b}_\sigma^{11}}{d_{W\sigma}} - \frac{\bar{a}_\sigma^1}{2}\right)u_\sigma^n\chi_{\{\sigma\in\varepsilon_W\cap\varepsilon_{\text{ext}}^{\text{DBC}}\}}m(\sigma) \\ &+ \mathcal{k}\big(\bar{b}_{\sigma_{GC}}^{12}u_\sigma^n\chi_{\{W=ne\}} - \bar{b}_{\sigma_{GC}}^{12}u_\sigma^n\chi_{\{W=nw\}} \\ &\quad + \bar{b}_{\sigma_{GC}}^{12}u_\sigma^n\chi_{\{W=sw\}} - \bar{b}_{\sigma_{GC}}^{12}u_\sigma^n\chi_{\{W=se\}}\big)\end{aligned} \tag{61}$$

where $W \in \mathcal{T}_h$ and u_W^{n-1} is the value of the piecewise constant function $u_{h,\mathcal{k}}^{n-1}$ in W. The equality (60) represents a system of $N_x \times N_y$ linear equations where

$N_x \times N_y = \mathrm{card}(\mathcal{T}_h)$. If we multiply $\mathcal{L}_h(u^n_{h,\mathcal{K}})$ by u^n_W, sum over all $W \in \mathcal{T}_h$ and split into three parts A, B and C we obtain

$$\sum_{W\in\mathcal{T}_h} \mathcal{L}_h(u^n_{h,\mathcal{K}})u^n_W = A + B + C \tag{62}$$

where

$$A = (1+r\mathcal{K}) \sum_{W\in\mathcal{T}_h} \left(u^n_W\right)^2 m(W) = (1+r\mathcal{K})||u^n_{h,\mathcal{K}}||^2_{L_2(\Omega)} \tag{63}$$

$$\begin{aligned} B = {} & \mathcal{K} \sum_{W\in\mathcal{T}_h} u^n_W \sum_{\sigma\in\varepsilon_W\cap\varepsilon_{\mathrm{int}}} -\Phi^n_\sigma(u^n_{h,\mathcal{K}})m(\sigma) + \mathcal{K} \sum_{W\in\mathcal{T}_h} u^n_W \sum_{\sigma\in\varepsilon_W\cap\varepsilon^{\mathrm{DBC}}_{\mathrm{ext}}} \frac{\bar{b}^{11}_\sigma}{d_{W\sigma}} u^n_W m(\sigma) \\ & + \frac{\mathcal{K}}{2}\left[\bar{b}^{12}_{\sigma_{GC}}(u^n_W)^2\right]^{ne}_{nw} + \frac{\mathcal{K}}{2}\left[\bar{b}^{12}_{\sigma_{GC}}(u^n_W)^2\right]^{sw}_{se} \end{aligned} \tag{64}$$

$$C = \mathcal{K} \sum_{W\in\mathcal{T}_h} u^n_W \sum_{\sigma\in\varepsilon_W\cap\varepsilon_{\mathrm{int}}} \Psi^n_\sigma(u^n_{h,\mathcal{K}})m(\sigma) - \mathcal{K} \sum_{W\in\mathcal{T}_h} u^n_W \sum_{\sigma\in\varepsilon_W\cap\varepsilon^{\mathrm{DBC}}_{\mathrm{ext}}} \frac{\bar{a}^1_\sigma}{2} u^n_W m(\sigma) \tag{65}$$

Terms in the second row of (64) have been derived by replacing all u_N, u_S by their reconstructions (36) and (37) and exploiting constant extrapolation property (24) $\forall\sigma \in \varepsilon^{\mathrm{GCE}}_{\mathrm{ext}}$ (for more details see Remark 2). In this context the notation $[u^n_W]^x_y$ means $[u^n_W]^x_y = u^n_x - u^n_y$.

Our next goal is to find a positive lower bound for the terms $A+B+C$. In order to rewrite the expression B let us recall a common finite volume technique trick for anti-symmetric $\Phi^n_{\sigma_{EW}}(u^n_{h,\mathcal{K}}) = -\Phi^n_{\sigma_{WE}}(u^n_{h,\mathcal{K}})$, namely:

$$\sum_{W\in\mathcal{T}_h} u^n_W \sum_{\sigma\in\varepsilon_W\cap\varepsilon_{\mathrm{int}}} \Phi^n_{\sigma_{WE}}(u^n_{h,\mathcal{K}}) = \sum_{\sigma\in\varepsilon_{\mathrm{int}}} \Phi^n_{\sigma_{WE}}(u^n_{h,\mathcal{K}})u^n_W \tag{66}$$

$$\sum_{W\in\mathcal{T}_h} u^n_W \sum_{\sigma\in\varepsilon_W\cap\varepsilon_{\mathrm{int}}} \Phi^n_{\sigma_{WE}}(u^n_{h,\mathcal{K}}) = \sum_{\sigma\in\varepsilon_{\mathrm{int}}} -\Phi^n_{\sigma_{WE}}(u^n_{h,\mathcal{K}})u^n_E. \tag{67}$$

Summing (66) and (67) and dividing it by 2 gives us the following identity:

$$\sum_{W\in\mathcal{T}_h} u^n_W \sum_{\sigma\in\varepsilon_W\cap\varepsilon_{\mathrm{int}}} \Phi^n_{\sigma_{WE}}(u^n_{h,\mathcal{K}}) = \frac{1}{2}\sum_{\sigma\in\varepsilon_{\mathrm{int}}} -\Phi^n_{\sigma_{WE}}(u^n_{h,\mathcal{K}})(u^n_E - u^n_W). \tag{68}$$

Using this identity one can formulate the following equality:

$$\mathcal{K} \sum_{W\in\mathcal{T}_h} u^n_W \sum_{\sigma\in\varepsilon_W\cap\varepsilon_{\mathrm{int}}} -\Phi^n_\sigma(u^n_{h,\mathcal{K}})m(\sigma) = \frac{\mathcal{K}}{2}\sum_{\sigma\in\varepsilon_{\mathrm{int}}} \Phi^n_\sigma(u^n_{h,\mathcal{K}})\frac{u^n_E - u^n_W}{d_{EW}} d_{EW} m(\sigma) \tag{69}$$

Let us now analyze the sum $\sum_{\sigma\in\varepsilon_{\mathrm{int}}} \Phi^n_\sigma(u^n_{h,\mathcal{K}})\frac{u^n_E-u^n_W}{d_{EW}}$ appearing in (69). We can bound it from bellow as follows:

$$\begin{aligned} \sum_{\sigma\in\varepsilon_{\mathrm{int}}} \Phi^n_\sigma(u^n_{h,\mathcal{K}})\frac{u^n_E - u^n_W}{d_{EW}} &= \sum_{\sigma\in\varepsilon_{\mathrm{int}}} \left(\bar{b}^{11}_\sigma \frac{u^n_E - u^n_W}{d_{EW}} + \bar{b}^{12}_\sigma \frac{u^n_N - u^n_S}{d_{NS}}\right)\frac{u^n_E - u^n_W}{d_{EW}} \\ &\geq \sum_{\sigma\in\varepsilon_{\mathrm{int}}} \bar{b}^{11}_\sigma \left(\frac{u^n_E - u^n_W}{d_{EW}}\right)^2 - \left|\sum_{\sigma\in\varepsilon_{\mathrm{int}}} \bar{b}^{12}_\sigma \frac{u^n_N - u^n_S}{d_{NS}}\frac{u^n_E - u^n_W}{d_{EW}}\right| \end{aligned} \tag{70}$$

Applying Young's inequality in the second term of (70) leads to

$$\left|\sum_{\sigma\in\varepsilon_{\mathrm{int}}} \bar{b}^{12}_\sigma \frac{u^n_N - u^n_S}{d_{NS}}\frac{u^n_E - u^n_W}{d_{EW}}\right| \leq \sum_{\sigma\in\varepsilon_{\mathrm{int}}} \frac{1}{2}\left[\left(\frac{u^n_E - u^n_W}{d_{EW}}\right)^2 + \left(\frac{\bar{b}^{12}_\sigma}{\bar{b}^{11}_\sigma}\right)^2 \left(\frac{u^n_N - u^n_S}{d_{NS}}\right)^2\right]\bar{b}^{11}_\sigma.$$

Since our diffusion tensor $\mathbf{B}$ is smooth and positive definite we can use, for h_x, h_y sufficiently small, the following estimate

$$\sum_{\sigma\in\varepsilon_{\text{int}}}\left(\frac{\bar{b}^{12}_{\sigma}}{\bar{b}^{11}_{\sigma}}\right)^2\left(\frac{u^n_N-u^n_S}{d_{NS}}\right)^2\bar{b}^{11}_{\sigma}\leq\gamma\sum_{\sigma\in\varepsilon_{\text{int}}}\left(\frac{u^n_E-u^n_W}{d_{EW}}\right)^2\bar{b}^{11}_{\sigma} \tag{71}$$

where $0\leq\gamma<1$ (cf. [6]). Combining expressions (69)-(71) leads to

$$\frac{\kappa}{2}\sum_{\sigma\in\varepsilon_{\text{int}}}\Phi^n_{\sigma}(u^n_{h,\kappa})\frac{u^n_E-u^n_W}{d_{EW}}d_{EW}m(\sigma)\geq\frac{\kappa}{2}\left(\frac{1-\gamma}{2}\right)\sum_{\sigma\in\varepsilon_{\text{int}}}\bar{b}^{11}_{\sigma}\frac{(u^n_E-u^n_W)^2}{d_{EW}}m(\sigma). \tag{72}$$

Concerning the second sum in (64) we can rewrite it as follows:

$$\kappa\sum_{W\in\mathcal{T}_h}u^n_W\sum_{\sigma\in\varepsilon_W\cap\varepsilon^{\text{DBC}}_{\text{ext}}}\frac{\bar{b}^{11}_{\sigma}}{d_{W\sigma}}u^n_W m(\sigma)=\kappa\sum_{\sigma\in\varepsilon^{\text{DBC}}_{\text{ext}}}\bar{b}^{11}_{\sigma}\frac{(u^n_W)^2}{d_{W\sigma}}m(\sigma) \tag{73}$$

Similarly to the previous analysis let us now expand the terms appearing in (65). Since the advection-associated flux term $\Psi^n_{\sigma}(u^n_{h,\kappa})$ is symmetric, i.e. $\Psi^n_{\sigma_{WE}}(u^n_{h,\kappa})=\Psi^n_{\sigma_{EW}}(u^n_{h,\kappa})$ we can rewrite the first sum in (65) as follows:

$$\begin{aligned}\kappa\sum_{W\in\mathcal{T}_h}u^n_W\sum_{\sigma\in\varepsilon_W\cap\varepsilon_{\text{int}}}\Psi^n_{\sigma}(u^n_{h,\kappa})m(\sigma)&=\frac{\kappa}{2}\sum_{\sigma\in\varepsilon_{\text{int}}}\Psi^n_{\sigma}(u^n_{h,\kappa})(u^n_E+u^n_W)m(\sigma)\\&=\frac{\kappa}{2}\sum_{\sigma\in\varepsilon_{\text{int}}}\bar{a}^1_{\sigma}\frac{(u^n_E)^2-(u^n_W)^2}{2}m(\sigma)\end{aligned} \tag{74}$$

The second sum in (65) can be treated analogically to (73):

$$-\kappa\sum_{W\in\mathcal{T}_h}u^n_W\sum_{\sigma\in\varepsilon_W\cap\varepsilon^{\text{DBC}}_{\text{ext}}}\frac{\bar{a}^1_{\sigma}}{2}u^n_W m(\sigma)=-\kappa\sum_{\sigma\in\varepsilon^{\text{DBC}}_{\text{ext}}}\bar{a}^1_{\sigma}\frac{(u^n_W)^2}{2}m(\sigma) \tag{75}$$

Switching temporarily from local basis to standard basis notation one can formulate the following identity:

$$\begin{aligned}&\frac{\kappa}{2}\sum_{\sigma\in\varepsilon_{\text{int}}}\bar{a}^1_{\sigma}\frac{(u^n_E)^2-(u^n_W)^2}{2}m(\sigma)-\frac{\kappa}{2}\sum_{\sigma\in\varepsilon^{\text{DBC}}_{\text{ext}}}\bar{a}^1_{\sigma}\frac{(u^n_W)^2}{2}m(\sigma)\\&-\frac{\kappa}{2}\sum_{\sigma\in\varepsilon^{\text{GCE}}_{\text{ext}}}\bar{a}^1_{\sigma}\frac{(u^n_W)^2}{2}m(\sigma)=\frac{\kappa}{4}\sum_{p\in\mathcal{T}_h}\left[\left(a^1_{pw}-a^1_{pe}\right)h_y+\left(a^2_{ps}-a^2_{pn}\right)h_x\right](u^n_p)^2\\&=\frac{\kappa}{4}\sum_{p\in\mathcal{T}_h}(u^n_p)^2\sum_{q\in N(p)}-\vec{A}_{pq}\cdot\vec{n}_{pq}m(\sigma_{pq})=-\frac{\kappa}{4}\sum_{p\in\mathcal{T}_h}(u^n_p)^2\int_{\partial p}\vec{A}\cdot\vec{n}_p\,\mathrm{d}\gamma\\&=-\frac{\kappa}{4}\sum_{p\in\mathcal{T}_h}(u^n_p)^2\int_p\nabla\cdot\vec{A}\,\mathrm{d}x=-\frac{\kappa}{4}\int_{\Omega}\nabla\cdot\vec{A}(u^n_{h,\kappa})^2\,\mathrm{d}x=-\frac{\kappa}{4}\kappa||u^n_{h,\kappa}||^2_{L_2(\Omega)}\end{aligned} \tag{76}$$

where in the last equality we have expolited the form of the advection vector (16). Inserting this result back into (65) gives us

$$C=-\frac{\kappa}{4}\kappa||u^n_{h,\kappa}||^2_{L_2(\Omega)}-\frac{\kappa}{2}\sum_{\sigma\in\varepsilon^{\text{DBC}}_{\text{ext}}}\frac{\bar{a}^1_{\sigma}}{2}(u^n_W)^2m(\sigma)+\frac{\kappa}{2}\sum_{\sigma\in\varepsilon^{\text{GCE}}_{\text{ext}}}\frac{\bar{a}^1_{\sigma}}{2}(u^n_W)^2m(\sigma) \tag{77}$$

By introducing $\hat{\beta} = \left(r - \frac{\kappa}{4}\right)$ and $\hat{\eta} = \left(\frac{1-\gamma}{4}\right)$ and inserting (72), (73) and (77) into (62) we obtain

$$\begin{aligned}\sum_{W\in\mathcal{T}_h}\mathcal{L}_h(u^n_{h,\mathcal{k}})u^n_W \geq\ & (1+\mathcal{k}\hat{\beta})||u^n_{h,\mathcal{k}}||^2_{L_2(\Omega)} + \mathcal{k}\hat{\eta}\sum_{\sigma\in\varepsilon_{\text{int}}}\bar{b}^{11}_\sigma\frac{(u^n_E-u^n_W)^2}{d_{EW}}m(\sigma)\\ &+\mathcal{k}\sum_{\sigma\in\varepsilon^{\text{DBC}}_{\text{ext}}}\bar{b}^{11}_\sigma\frac{(u^n_W)^2}{d_{W\sigma}}m(\sigma)+\frac{\mathcal{k}}{2}\left[\bar{b}^{12}_{\sigma_{GC}}(u^n_W)^2\right]^{nw}_{ne}+\frac{\mathcal{k}}{2}\left[\bar{b}^{12}_{\sigma_{GC}}(u^n_W)^2\right]^{se}_{sw}\\ &-\frac{\mathcal{k}}{2}\sum_{\sigma\in\varepsilon^{\text{DBC}}_{\text{ext}}}\frac{\bar{a}^1_\sigma}{2}(u^n_W)^2m(\sigma)+\frac{\mathcal{k}}{2}\sum_{\sigma\in\varepsilon^{\text{GCE}}_{\text{ext}}}\frac{\bar{a}^1_\sigma}{2}(u^n_W)^2m(\sigma).\end{aligned}\tag{78}$$

For the sake of brief notation let us define following magnitudes:

$$\begin{aligned}&\bar{b}^{11}_{\min}=\min_{\sigma\in\varepsilon_{\text{int}}}\bar{b}^{11}_\sigma,\ \bar{b}^{11}_{\max}=\max_{\sigma\in\varepsilon}\bar{b}^{11}_\sigma,\ \bar{b}^{12}_{\max}=\max_{\sigma\in\varepsilon^{\text{GCE}}_{\text{ext}}}|\bar{b}^{12}_\sigma|,\ \bar{a}^1_{\max}=\max_{\sigma\in\varepsilon}|\bar{a}^1_\sigma|,\\ &h_{\min}=\min(h_x,h_y),\ h_{\max}=\max(h_x,h_y).\end{aligned}$$

We also introduce the set $\Upsilon=\{nw,ne,sw,se\}$ which includes all four corner cells of the domain Ω. Then, the inequality (78) can be further simplified as follows:

$$\begin{aligned}\sum_{W\in\mathcal{T}_h}\mathcal{L}_h(u^n_{h,\mathcal{k}})u^n_W \geq\ & \left(1+\mathcal{k}r-\mathcal{k}\frac{\kappa}{4}\right)||u^n_{h,\mathcal{k}}||^2_{L_2(\Omega)}+\mathcal{k}\eta|u^n_{h,\mathcal{k}}|^2_{1,\mathcal{T}_h}\\ &+\mathcal{k}\bar{b}^{11}_{\min}\sum_{\sigma\in\varepsilon^{\text{DBC}}_{\text{ext}}}\frac{(u^n_W)^2}{d_{W\sigma}}m(\sigma)-\mathcal{k}\sum_{W\in\Upsilon}\frac{|\bar{b}^{12}_{\sigma_{GC}}|}{2}(u^n_W)^2-\mathcal{k}\sum_{\sigma\in\varepsilon^{\text{DBC}}_{\text{ext}}}\frac{|\bar{a}^1_\sigma|}{4}(u^n_W)^2m(\sigma)\\ &-\mathcal{k}\sum_{\sigma\in\varepsilon^{\text{GCE}}_{\text{ext}}}\frac{|\bar{a}^1_\sigma|}{4}(u^n_W)^2m(\sigma)\geq(1+\mathcal{k}\beta)\,||u^n_{h,\mathcal{k}}||^2_{L_2(\Omega)}\end{aligned}\tag{79}$$

with $\eta=\hat{\eta}\,\bar{b}^{11}_{\min}$ and $\beta=\hat{\beta}-\frac{\bar{b}^{12}_{\max}}{2m(p)}-\frac{\bar{a}^1_{\max}}{2h_{\min}}$. In order guarantee positivity of (79) it is sufficient to insist that

$$1+\mathcal{k}\beta>0.\tag{80}$$

In case β is positive, relation (80) always holds, however if β is negative, (80) is equivalent to insisting that $\mathcal{k}<-1/\beta$. Hence one can derive the following restriction on the time-step-size $\mathcal{k}$:

$$\mathcal{k}<\frac{4m(p)}{(\kappa-4r)\,m(p)+2\bar{b}^{12}_{\max}+2\bar{a}^1_{\max}h_{\max}}\tag{81}$$

Assuming $\beta<0$ and (81) holds, we get from (79) for any $u^n_{h,\mathcal{k}}\in\mathcal{P}_0(\mathcal{T}_h)$ that

$$\sum_{p\in\mathcal{T}_h}\mathcal{L}_h(u^n_{h,\mathcal{k}})u^n_p\geq\alpha||u^n_{h,\mathcal{k}}||^2_{L_2(\Omega)}\tag{82}$$

with $\alpha=1+\mathcal{k}\beta>0$. Let us summarize the existence and uniqueness of the numerical solution of the scheme (38) in the following theorem.

Theorem 2.3 (Existence and Uniqueness)**.** *Let $\mathcal{T}_h$ be an admissible mesh on the domain Ω and let $h_x>0, h_y>0$ be sufficiently small. Let the time step satisfy the condition (81). Then the unique solution $u^n_{h,\mathcal{k}}\in\mathcal{P}_0(\mathcal{T}_h)$ to the equation (38) exists.*

Proof. Assume that u_p, $p \in \mathcal{T}_h$, satisfy the linear system (60) with a zero right-hand side, i.e. that $f_{h,\mathcal{k}}(u^{n-1}_{h,\mathcal{k}}) = 0,\ \forall p \in \mathcal{T}_h$. Then due to the relation (82)

$$\alpha ||u^n_{h,\mathcal{k}}||^2_{L_2(\Omega)} \leq \sum_{p\in\mathcal{T}_h} \mathcal{L}_h(u^n_{h,\mathcal{k}})u^n_p = \sum_{p\in\mathcal{T}_h} f_{h,\mathcal{k}}(u^{n-1}_{h,\mathcal{k}})u^n_p = 0. \tag{83}$$

Since both, the relation (83) and strict positivity of α, must hold, we deduce that $u^n_p = 0,\ \forall p \in \mathcal{T}_h$. It means that the kernel of the homogeneous linear system $\mathcal{L}_h(u^n_{h,\mathcal{k}}) = 0$ contains only zero vector which implies that the matrix is regular. Since regular system matrix implies that there exists a unique solution to (60) the proof is complete. □

Remark 2. Without loss of generality let us concentrate on the finite volumes surrounding the ghost cell boundary located to the north of the domain Ω. If we multiply the corresponding terms in the second and third row of (59) by u^n_W, sum over $\forall W \in \mathcal{T}_h$ and note that the two rows of finite volumes around the northern boundary consist of $p_{1,N_y}, p_{2,N_y}, \ldots, p_{N_x,N_y}$ and $p_{1,N_y+1}, p_{2,N_y+1}, \ldots, p_{N_x,N_y+1}$ we can write

$$\begin{aligned}
&-\mathcal{k}\bar{b}^{12}_{\sigma_{GC}} u^n_{nw} u^n_S + \mathcal{k} \sum_{W\in\mathcal{T}_h} u^n_W \sum_{\substack{\sigma\in\varepsilon_W\cap \\ (\varepsilon^{\mathrm{GCE}}_{\mathrm{ext}}\setminus\varepsilon^{\mathrm{GCE}}_{\mathrm{cor}})}} \bar{b}^{12}_{\sigma}\,(u^n_N - u^n_S) + \mathcal{k}\bar{b}^{12}_{\sigma_{GC}} u^n_{ne} u^n_N = \\
&-\mathcal{k}\bar{b}^{12}_{\sigma_{GC}} u^n_{p_{1,N_y}} \frac{2u^n_{p_{1,N_y}} + 2u^n_{p_{2,N_y}}}{4} + \mathcal{k}\bar{b}^{12}_{\sigma_{GC}} u^n_{p_{2,N_y}} \left(\frac{2u^n_{p_{1,N_y}} + 2u^n_{p_{2,N_y}}}{4} \right. \\
&\left. - \frac{2u^n_{p_{2,N_y}} + 2u^n_{p_{3,N_y}}}{4} \right) + \mathcal{k}\bar{b}^{12}_{\sigma_{GC}} u^n_{p_{3,N_y}} \left(\frac{2u^n_{p_{2,N_y}} + 2u^n_{p_{3,N_y}}}{4} \right. \\
&\left. - \frac{2u^n_{p_{3,N_y}} + 2u^n_{p_{4,N_y}}}{4} \right) + \cdots + \mathcal{k}\bar{b}^{12}_{\sigma_{GC}} u^n_{p_{N_x,N_y}} \frac{2u^n_{p_{N_x-1,N_y}} + 2u^n_{p_{N_x-1,N_y}}}{4} \\
&= \frac{\mathcal{k}}{2} \left(-\bar{b}^{12}_{\sigma_{GC}} (u^n_{p_{1,N_y}})^2 + \bar{b}^{12}_{\sigma_{GC}} (u^n_{p_{N_x,N_y}})^2 \right)
\end{aligned} \tag{84}$$

Note that in the course of reconstruction of the boundary terms u^n_N, u^n_S by (36) we have also exploited the constant extrapolation property (24).

3. **Numerical Experiment.** In this section we performed a numerical experiment to check the accuracy and rate of convergence of our scheme (38). In order to measure the accuracy and rate of convergence of our scheme we use as a benchmark the quasi closed-form solution for a European call option derived by Heston in [12]. Other useful source is the book of Gatheral (cf. [11]) or Kútik's disseration thesis (cf. [14]).

We applied our scheme on the evolution of the initial profile described by (4) with the coupling $\mathcal{k} = h_x h_y$. We also computed the theoretical upper bound for the time-step-size due to (81), cf. fifth column in Table 2. Note that even though the condition is not met for the coarsest grid we did not encounter any problems when generating the numerical solution. This may indicate that the condition (81) is too restrictive. Furthermore as indiciated in the last two columns of the Table 2 using a fine mesh the scheme exhibits an error of order 10^{-5} in the $L_2(I,\Omega)$ norm and a second order experimental rate of convergence. We should also note that the main drawback of this scheme is that the solution slightly deceeds zero near the strike

price region ($S = E$), although it should stay in the range from $\tau = 0$. Table 1 lists all parameters and variable ranges used in this section.

TABLE 1. Variable ranges and parameter values used for the computation of the numerical solution for the Heston model (3)

Parameter	Value	Parameter	Value
x	$[-7, 3]$	S	$[0.1, 2008]$
y	$[0, 1]$	v	$[0, 1]$
τ	$[0, 0.05]$	t	$[0, 0.05]$
E	100	r	0.1
ρ	-0.5	κ	5
θ	0.07	σ	0.5
λ	0	T	0.05

TABLE 2. Errors in $L_2(I, \Omega)$ norm and EOCs of the scheme (38) for the exact solution of the Heston model.

N_x	N_y	N_{ts}	$\mathcal{k}$	upper bound (81)	$\|\|\text{error}\|\|_{L_2(I,\Omega)}$	EOC
20	10	1	0.05	0.0381	$1.341 \ \ 10^{-3}$	-
40	20	4	0.0125	0.0185	$5.491 \ \ 10^{-4}$	1.29
80	40	16	0.003125	$8.573 \ \ 10^{-3}$	$1.952 \ \ 10^{-4}$	1.49
160	80	64	$7.812 \ \ 10^{-4}$	$3.674 \ \ 10^{-3}$	$6.118 \ \ 10^{-5}$	1.67
320	160	256	$1.953 \ \ 10^{-4}$	$1.422 \ \ 10^{-3}$	$1.729 \ \ 10^{-5}$	1.82

4. **Conclusions.** In this article we proposed a numerical scheme based on the finite volume technique for solving the linear partial differential equation arising in the Heston model. We used logarithmic transformation to simplify the equation and obtain a divergent form of two-dimensional diffusion tensor. We further expanded the advection term into conservative and nonconservative part and applied Green's theorem onto the integrated governing equation. Next we dealt with the issue of numerical implementation of the boundary conditions. For the zero variance boundary the Fichera condition was taken into account and a solution extrapolation to the ghost-cells was made. Special attention was devoted to the solvability of the system of equations in each time step. We proved a theorem which states that under certain conditions an unique numerical solution does exist. Finally we examined the accuracy and experimental rate of convergence of the scheme on a numerical experiment with an exact solution.

Acknowledgments. This work was supported by the grant APVV-0184-10 and VEGA 1/1137/12. We thank Daniel Ševčovič for discussions about the Fichera condition.

REFERENCES

[1] L. Andersen, *Simple and efficient simulation of the Heston stochastic volatility model*, Journal of Computational Finance 11, **3** (2008), 1–42.

[2] F. Black and and M. Scholes, *The pricing of options and corporate liabilities*, The Journal of Political Economy 81, **3** (1973), 637–654.

[3] R. Cont, *Empirical properties of asset returns: stylized facts and statistical issues*, Quantitative Finance 1, **2** (2001), 223–236.

[4] Y. Coudiere, J. P. Vila and P. Villedieu, *Convergence rate of a finite volume scheme for a two-dimensional convection-diffusion problem*, M2AN Math. Model. Numer. Anal. 33, (1999), 493–516.

[5] J. Cox, J. Ingersoll and S. Ross, *A theory of the term structure of interest rates*, Econometrica 53, **2** (1985), 385–407.

[6] O. Drblíková and K. Mikula, *Convergence analysis of finite volume scheme for nonlinear tensor anisotropic diffusion in image processing*, SIAM Journal on Numerical Analysis 46, **1** (2007), 37–60.

[7] R. Eymard, T. Gallouët and R. Herbin, " Finite Volume Methods," in: Handbook Of Numerical Analysis, Elsevier Science B.V., Amsterdam, 2000.

[8] G. Fichera, *Sulle equazioni differenziali lineari ellittico-paraboliche del secondo ordine*, Atti Accad. Naz. Lincei, Mem., Cl. Sci. Fis. Mat. Nat., Sez. I, VIII., **5** (1956), 3–30.

[9] P. A. Forsyth, K. R. Vetzal and R. Zvan, *A finite element approach to the pricing of discrete lookbacks with stochastic volatility*, Applied Mathematical Finance, **6** (1998), 87–106.

[10] P. Frolkovič and K. Mikula, *High-resolution flux-based level set method*, SIAM Journal on Scientific Computing 29, **2** (2007), 579–597.

[11] J. Gatheral, " The Volatility Surface: A Practitioner's Guide," John Wiley & Sons, Inc., New Jersey, 2006.

[12] S. L. Heston, *A closed-form solution for options with stochastic volatility with applications to bond and currency options*, The Review of Financial Studies 6, **2** (1993), 327–343.

[13] K. J. In't Hout and S. Foulon, *ADI finite difference schemes for option pricing in the Heston model with correlation*, Internation Journal of Numerical Analysis and Modeling 7, **2** (2010), 303–320.

[14] P. Kútik, *Numerical solution of partial differential equations in financial mathematics*, PhD. Thesis, Slovak University of Technology, Bratislava, 2014.

[15] R. J. LeVeque, "Finite Volume Methods for Hyperbolic Problems," Cambridge University Press, Cambridge, 2002.

[16] R. Merton, *Theory of rational option pricing*, The Bell Journal of Economics and Management Science, (1973), 141–183.

[17] R. Zvan, P. A. Forsyth and K. R. Vetzal, *A finite volume approach for contingent claims valuation*, IMA J. Numer. Anal. 21, **3** (2001), 703—731.

Received xxxx 20xx; revised xxxx 20xx.

E-mail address: pavol.kutik@gmail.com
E-mail address: karol.mikula@gmail.com